



HAL
open science

Investigation of PM₁₀, PM_{2.5}, PM₁ in an unoccupied airflow-controlled room: How reliable to neglect resuspension and assume unreactive particles?

Evdokia Stratigou, Sébastien Dusanter, Joel Brito, Véronique Riffault

► To cite this version:

Evdokia Stratigou, Sébastien Dusanter, Joel Brito, Véronique Riffault. Investigation of PM₁₀, PM_{2.5}, PM₁ in an unoccupied airflow-controlled room: How reliable to neglect resuspension and assume unreactive particles?. *Building and Environment*, 2020, 186, pp.107357. 10.1016/j.buildenv.2020.107357 . hal-02975485

HAL Id: hal-02975485

<https://hal.science/hal-02975485v1>

Submitted on 17 Oct 2022

HAL is a multi-disciplinary open access archive for the deposit and dissemination of scientific research documents, whether they are published or not. The documents may come from teaching and research institutions in France or abroad, or from public or private research centers.

L'archive ouverte pluridisciplinaire **HAL**, est destinée au dépôt et à la diffusion de documents scientifiques de niveau recherche, publiés ou non, émanant des établissements d'enseignement et de recherche français ou étrangers, des laboratoires publics ou privés.



Distributed under a Creative Commons Attribution - NonCommercial 4.0 International License

1 **Investigation of PM₁₀, PM_{2.5}, PM₁ in an unoccupied airflow-controlled room:**
2 **how reliable to neglect resuspension and assume unreactive particles?**

3 **Evdokia STRATIGOU¹, Sébastien DUSANTER¹, Joel BRITO¹, Véronique RIFFAULT¹**

4
5 **¹ IMT Lille Douai, Univ. Lille, SAGE – Département Sciences de l'Atmosphère et Génie de**
6 **l'Environnement, F-59000 Lille, France**

7
8 Corresponding author: Prof. Véronique RIFFAULT, veronique.riffault@imt-lille-douai.fr

9 IMT Lille Douai – Douai Campus, 941 rue Charles Bourseul CS 10838, 59508 Douai cedex,
10 FRANCE

11 Tel: (33) 327 712 604 – Fax: (33) 327 712 914

12

13

14 **Abstract**

15 It is now well recognized that Particulate Matter (PM) is one of the main air pollutants affecting
16 both ambient and indoor air quality. While ambient PM mass concentration measurements are
17 often performed by air quality monitoring networks, current regulations do not address their
18 indoor concentrations. The latter can be estimated nonetheless from a mass balance analysis
19 accounting for (i) the transfer of particles from outdoor and (ii) their typical indoor sources
20 (emissions, resuspension) and sinks (deposition, removal by air exchange). Inherently, the mass
21 balance analysis is valid with inert atmospheric species, i.e. mass is conserved and described by
22 sources and sinks, thus assuming no physicochemical transformations. To check that the relative
23 imbalance (RI) is not significant over different size fractions, a series of careful measurements
24 were conducted in an unoccupied room within a building incorporating an energy-efficient design
25 (minimal heat losses, negligible air leaks, etc.). We show that by carefully characterizing the
26 room properties, i.e. the air exchange rate, penetration factors and deposition rates for sized-
27 resolved particles, the PM_{10} and $PM_{2.5}$ fractions, which are typically regulated outdoors, as well
28 as PM_1 , can be well estimated indoors (with RI between measured and expected values $< 19\%$)
29 under moderate ambient temperatures ($< 22^\circ\text{C}$ in this study). However, RI increases significantly,
30 especially for submicron particles, at higher temperatures, indicating possible transformations in
31 the particulate phase, which are not accounted for by the mass balance model. Therefore caution
32 is recommended regarding the mass balance analysis to estimate PM fractions indoors, especially
33 for PM_1 .

34

35 **Keywords:** Indoor Air Quality, Particle penetration, Particle deposition, Aerosol budget, Mass
36 balance

37 **1. Introduction**

38 The infiltration of outdoor pollution combined with a range of indoor sources emitting volatile
39 organic compounds (VOCs) and particulate matter (PM) tends to lead to a lower air quality
40 indoors than outdoors.¹ According to the World Health Organization (WHO) ² 3.8 million
41 premature deaths worldwide were attributable to household air pollution in 2016, accounting for
42 7.7% of the global mortality. The design of effective strategies aiming at reducing personal
43 exposure to harmful species requires a good assessment of pollutant concentrations in the indoor
44 environment, which in turn requires a good understanding of their sources, their sinks and all the
45 physicochemical processes leading to their transformations.

46 Among atmospheric pollutants, PM has been classified as carcinogenic for humans,³ and several
47 countries have set air quality standards on ambient mass concentrations of PM with an
48 aerodynamic diameter below 10 μm (PM_{10}) or 2.5 μm ($\text{PM}_{2.5}$, also known as fine particles). PM
49 of even smaller sizes, e.g. with a diameter lower than 1 μm (PM_1), is of particular interest since it
50 deposits more easily in the lower respiratory tract where it can penetrate into the circulatory
51 system, impacting other organs.^{4,5} Furthermore, PM_1 are observed at high number concentrations
52 compared to larger particles, leading to large surface areas that can carry adsorbed organic
53 pollutants to the circulatory system.⁶

54 To better understand the sources and properties of PM on indoor air, previous studies have been
55 generally conducted either in simplified environments such as experimental chambers⁷⁻¹² or
56 proxy rooms,¹³ or in real buildings. In the former case, the focus is mainly on the formation of

57 secondary pollutants while the latter is aiming at assessing the anthropogenic influence by
58 investigating the impact of specific activities (such as cooking, candle combustion, use of
59 cleaning products, etc.) on particle nucleation and growth,^{14–20} or by focusing on the possible
60 transformations and origin of indoor particles under occupied conditions.^{20–25} Interestingly, only
61 a few studies focus on the investigation of particle origin under unoccupied conditions in real
62 rooms, therefore there is often a lack of understanding of the building influence itself.^{23,26–29}

63 Indoor concentrations of particles are typically driven by several processes acting either as
64 sources or sinks as expressed in the mass balance model (Eq. 1).

$$65 \quad V \frac{dC_{in}}{dt} = \alpha P V C_{out} - (\alpha + K) V C_{in} + R + S \quad \{1\}$$

66 where C_{in} and C_{out} are the indoor and outdoor concentrations ($\mu\text{g m}^{-3}$), respectively, V the volume
67 of the test room (m^3), α the air exchange rate (h^{-1}), P the penetration factor (dimensionless), K the
68 deposition rate (h^{-1}), R the resuspension rate ($\mu\text{g h}^{-1}$) and S the net results of additional processes
69 acting as sources or sinks ($\mu\text{g h}^{-1}$). The latter can be due to either direct emissions from human
70 activities such as cooking or cleaning, as well as physicochemical transformations of existing
71 particles such as condensation, evaporation and chemical reactivity.

72 The first term on the right-hand side of Equation 1 can be considered as a source of particles
73 originating from outdoor due to air exchange. The second term represents an indoor sink due to
74 air exchange and deposition. The third term, resuspension, acts as a source mainly for particles
75 larger than $1 \mu\text{m}$. For smaller particles the resuspension is likely negligible because they are more
76 difficult to detach from the floor due to relatively higher adhesive forces compared to removal
77 forces.^{30–32} The last term, S , aggregates additional sources or sinks due to indoor activities as

78 mentioned above. The accuracy associated to indoor budgets of PM_x ($x = 1, 2.5, 10$) derived from
79 Equation 1 depends on how well each term can be characterized, which is extremely challenging
80 given their dependence on the particle size and their co-variability.³³

81 The mass balance equation (MBE) has been previously used in various studies to (i) estimate
82 indoor concentrations of particles based on observed outdoor concentrations, (ii) quantify some
83 parameters such as particle penetration, deposition, and resuspension rates,^{27,30–32,34–55} and (iii)
84 estimate the strength of indoor particle sources resulting from human activities.^{46,47,56–62} In most
85 of these studies however, two important simplifications are usually made: (i) particles are inert
86 species and their number concentration and size does not change and (ii) particle resuspension is
87 negligible under unoccupied conditions.

88 However, the size distribution of outdoor particles being transferred indoors could be impacted
89 by volatilization, condensation or coagulation processes due to a change in environmental
90 conditions. Interestingly, Abt et al.,⁴⁷ performed measurements of continuous particle size and
91 mass concentration indoors and outdoors in four nonsmoking households located in the
92 metropolitan Boston area during winter and summer. The authors used the MBE to determine the
93 source emission and infiltration rates for specific particle sizes, as well as the contribution of
94 outdoor and indoor sources to indoor particle levels. The results showed that particles in the size
95 range $0.2 - 10.0 \mu\text{m}$ can be estimated within a median relative error of 20-50% using outdoor
96 concentrations and time-activity data, while for smaller particles ($0.02 - 0.2 \mu\text{m}$) the relative error
97 increases to 107%. This underestimation of the model may be related to the large variability in
98 indoor concentrations of smaller particles due to the contribution of specific activities to indoor
99 particle levels (cooking). In addition, transformations of particles penetrating indoors have been
100 observed in some studies.^{43,57,59,63–66} For example Polidori et al., 2006⁵⁹ showed that 71-76% of

101 the organic carbon in $PM_{2.5}$ is most likely formed or emitted indoors rather than penetrating from
102 outdoors. Hodas and Turpin (2014)⁶³ estimated that changes in the organic aerosol mass indoors
103 due to shifts in the gas-to-particle partitioning can reach 11-27%, while Rim et al. (2016)
104 indicated that ignoring coagulation for the prediction of ultrafine particles clearly leads to an
105 underestimation of indoor concentrations. These observations challenge the assumption of
106 particles being inert species when the MBE is used.

107 Chan et al.⁶⁷ and Chithra and Nagendra⁶⁸ also performed measurements of particulate matter
108 indoors and outdoors ($PM_{2.5}$ in homes, and PM_1 , $PM_{2.5}$, PM_{10} in classrooms respectively), where
109 human activities took place. They both used indoor models based on MBE in order to
110 characterize indoor particles and/or source strengths of known indoor activities and subsequently
111 predict the indoor concentrations. However, assumptions or limitations such as excluding
112 processes of fine particles in the model (i.e. particle transformations and resuspension) were
113 made. The authors found a good agreement between measured and estimated $PM_{2.5}$
114 concentrations indoors when the human activities are well identified and characterized. However,
115 the latter showed that PM_1 and PM_{10} concentrations can be wrongly estimated by not including
116 reactivity and resuspension respectively in the model. From the above discussion, it is clear that
117 common assumptions in the use of the MBE, i.e. particles being inert species and particle
118 resuspension being negligible, need to be carefully reconsidered.

119 The objective of this work is to investigate whether the mass balance model described in
120 Equation 1, assuming in a first step unreactive species (no particle processing) and negligible
121 resuspension under unoccupied conditions (anthropogenic influence is negligible), could
122 accurately predict indoor concentrations of PM_x ($x = 1, 2.5, 10$) if the parameters in this equation
123 were accurately quantified for each PM size fraction, or whether physicochemical

124 transformations and resuspension need to be included in the model, unlike to what has been
125 mainly considered until recently. In this work, we first characterized each term of the mass
126 balance model (Eq. 1) for an empty room of a low-energy building (described in Sections 2.2 and
127 3.1), and we then used the MBE to investigate how indoor measurements of PM_x compare to
128 values inferred from the model constrained by particulate outdoor measurements (Sections 2.3
129 and 4). Subsequently, we investigate whether this approach can highlight physical and chemical
130 processes occurring in the room, and therefore if the equation can be applied directly in more
131 complex situations, as usually assumed.

132 **2. Materials and methods**

133 **2.1. Building and campaign description**

134 The measurement facility is located at the Institute Mines Telecom Lille Douai, on the Douai
135 Campus, in northern France. This facility is a wooden building, a so-called energy-efficient
136 building with the BBC label (“Bâtiment Basse Consommation”), which according to the French
137 thermal regulation RT2012 has a primary energy consumption of maximum 50 kWh of oil
138 equivalent per m^2 per year on average.⁶⁹ This type of building is representative of recent
139 constructions aiming at significantly reducing the carbon footprint from heating and hot water
140 production, and therefore represents a trend for future constructions.⁷⁰ The building is composed
141 of two similar rooms of approximately $12 m^2$ of surface area and 2.4 m height, leading to a
142 surface to volume ratio of $0.4 m^2/m^3$. Only one room (hereafter called “test room”) was used to
143 perform all the characterization experiments (quantification of the parameters shown in Eq. 1)
144 and the simultaneous indoor/outdoor particle measurements, with no air exchange between the
145 two rooms. The test room is equipped with a dual-flow wall unit with heat recovery (KWL EC 60

146 Pro, HELIOS) providing an air flow rate of $17 \text{ m}^3 \text{ h}^{-1}$. This system includes a G4 filter for the
147 efficient removal of coarse particles. Ventilation was kept on during the whole measurement
148 period. In order to achieve the standards of energy-efficient buildings, the building is equipped
149 with thermally efficient windows (triple-glazed with Argon filling and an aluminum frame) and
150 the walls and roof are composed of wood, and insulated using wood wool and fibers. The floor is
151 covered by linoleum on top of wood wool and an OSB board. The external door is made of 33-
152 mm thick aluminum profiles and a triple-glazed window. Given the negligible air leakage, each
153 term of the MBE can be accurately characterized.

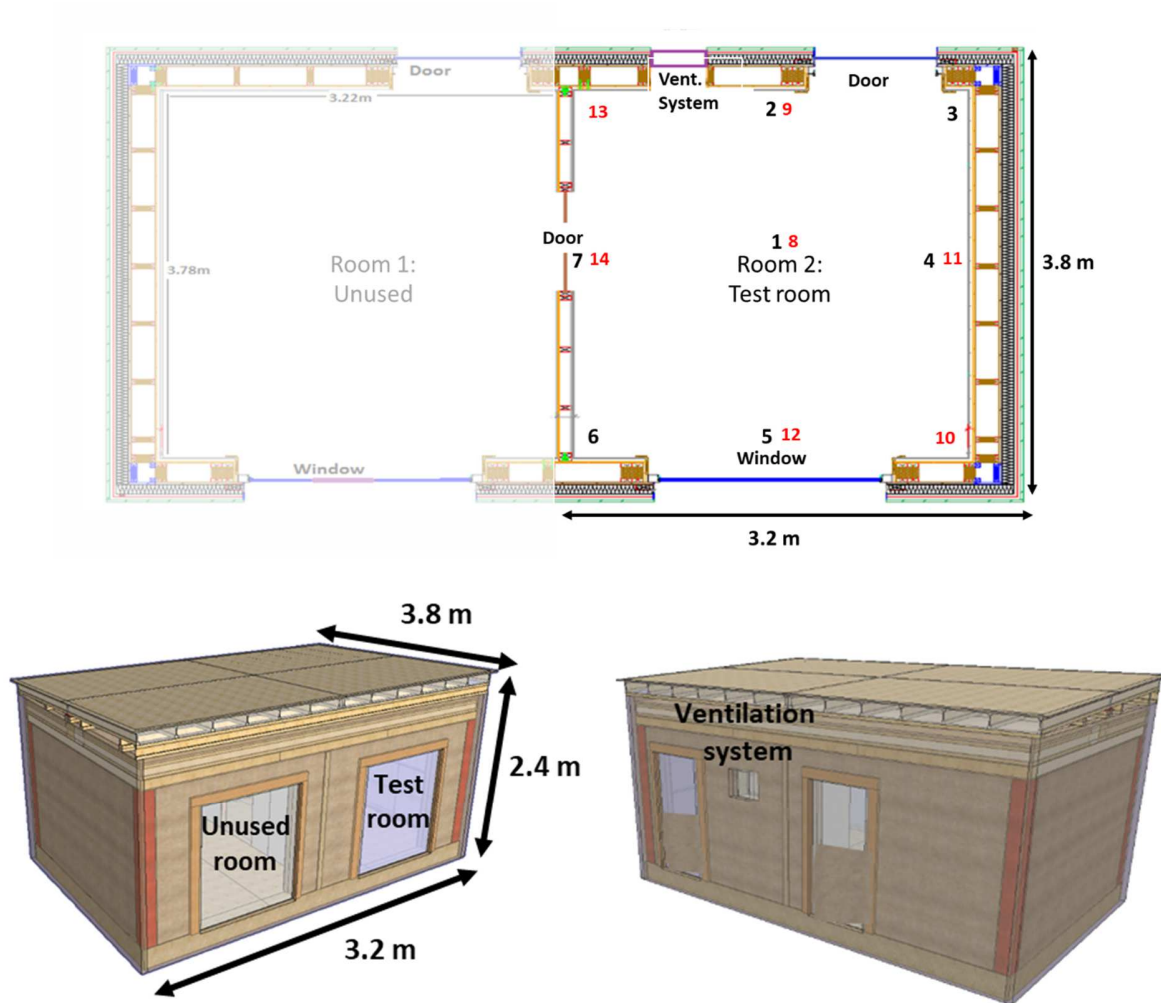
154 The experiments – including the characterization of P , α and K from Eq. 1 and indoor/outdoor
155 measurements of size-resolved particles – were conducted over a long time period from June
156 2016 to October 2017 to encompass a complete 1-year weather cycle. The test room was kept
157 unoccupied and unfurnished during the experiments to minimize resuspension and emissions.
158 Particulate matter measurements were performed using two optical particle counters (OPC,
159 AEROTRAK 8220, Table 1), sampling air at a flow rate of 2.8 L/min . Particle number
160 concentrations were acquired for five different size bins ($0.3\text{-}0.5$, $0.5\text{-}1.0$, $1.0\text{-}3.0$, $3.0\text{-}5.0$, 5.0-
161 $10.0 \mu\text{m}$) at a time resolution of 10 s . A larger size bin (for particles larger than $10 \mu\text{m}$) has been
162 discarded due to very low counts. The two OPCs were cross-calibrated before, during, and after
163 the measurement campaign (see section 1 in the Supplementary Information). Collocated
164 measurements from the two OPC indicate deviations lower than 14% for all size bins. For
165 indoor/outdoor measurement periods, the two OPC were used simultaneously to record size-
166 resolved C_{in} and C_{out} to test equation 1.

167 Table 1: Instrumentation information.

Instrument	Parameter	Specifications
TSI AEROTRAK Handheld Particle Counter 8220	Particle number concentration for 6 size bins (from 0.3 to >10.0 μm)	Counting efficiencies: 50% \pm 10% at 0.3 μm ; 100% by 0.45 μm ; 50% \pm 20% at all calibration cut sizes
Testo 480 probe	CO ₂ concentration	Range: 0 to 10,000 ppm

168

169 The spatial homogeneity of sized-resolved PM number concentrations within the test room was
 170 investigated to ensure that local measurements performed at the center of the test room would be
 171 representative of its whole volume, which is a prerequisite to constrain Eq. 1 with local
 172 measurements of C_{in} . It was assessed by keeping one OPC at a fixed reference point (#1 in
 173 Figure 1) and moving the other to 13 different locations within the test room (#2-13 in Figure 1).
 174 Each location was sampled for approximately 3 hours allowing particle counts to be
 175 intercompared for each pair. The relative difference was less than 12% across the five different
 176 size ranges, which is similar to differences observed when the two OPC performed collocated
 177 measurements (14%), thus confirming a homogeneous PM distribution in the test room. Detailed
 178 results are presented in section 2 of the SI.



179 Figure 1. 2-D and 3-D schematic diagrams of the building and positions of the OPCs.

180 Measurements performed at heights of 0.60 and 1.30 m are in black and red, respectively.

181

182 2.2. Determination of the Mass Balance Equation (MBE) parameters

183 The air exchange rate was measured according to the ASTM E741-00 method⁷¹ using CO₂ (Air

184 Liquide) as a tracer. Approximately 2,500 ppm (at the peak) of CO₂ was injected in the test room

185 and fast mixing was ensured using a fan during injection. CO₂ was measured using a Testo 480

186 probe (Table 1) at a time resolution of 20 seconds during the subsequent 15 hours, which was
187 long enough to reach its outdoor background concentration. The air exchange rate α (h^{-1}) was
188 derived from the CO_2 temporal decay, using the slope of a linear regression between the natural
189 logarithm of indoor CO_2 and time as shown in Equation 2:

$$190 \quad \ln[C_{\text{CO}_2}(t) - C_{\text{CO}_2,\text{bkg}}] = -\alpha \cdot t + \ln[C_{\text{CO}_2}(0) - C_{\text{CO}_2,\text{bkg}}] \quad \{2\}$$

191 where C_{CO_2} and $C_{\text{CO}_2,\text{bkg}}$ are the indoor air and background CO_2 mixing ratios (ppm), respectively,
192 α the air exchange rate (h^{-1}), and t the time (h).

193 The penetration factor (P) refers to the fraction of particles in the ambient air that passes through
194 the building shell and ventilation systems.^{36,72,73} Since the chosen building is tightly sealed to
195 meet energy-efficient standards, particles found indoor are assumed to be transported solely
196 through the ventilation system. In this study, particle concentrations measured simultaneously at
197 the entrance (i.e. outdoor) and exit (i.e. indoor) of the ventilation system were used in Equation 3
198 to quantify the penetration factor for each particle size bin.

$$199 \quad P = \frac{C_{\text{in,vent}}}{C_{\text{out}}} \quad \{3\}$$

200 where $C_{\text{in,vent}}$ and C_{out} are the particle number concentrations ($\# \text{ m}^{-3}$) exiting the ventilation
201 system indoors and outdoors, respectively. The initial 30 minutes of measurements were
202 discarded to prevent contamination from resuspension while setting the instruments. It is worth
203 noting that another existing (indirect) approach to determine penetration factors relies on using
204 the MBE while assuming no direct emissions of particles indoors.⁷⁴ However a major caveat
205 from this method is that it prevents any truly independent test of the MBE. Furthermore,

206 uncertainties from all other constrained parameters would propagate into the derived penetration
207 factor.

208 Measurements of penetration factors were conducted twice for a duration of minimum 12 hours
209 each, at the beginning (October 2016) and toward the end (June 2017) of the measurement
210 campaign (see Supplementary Information, Table S2). For a given measurement period and
211 despite sometimes large variations of the average outdoor concentrations (from 9 to 85%
212 depending on the size fraction, likely linked to changing ambient conditions of temperature,
213 humidity as well as particle composition, mixing state and phase), the penetration factor stays
214 quite stable without being affected by the outdoor situation (standard deviation less than 13%,
215 except for the larger size bin). When comparing the two periods, additional clogging of the air
216 filter as well as lower number concentrations led to higher relative standard deviations for the
217 larger size fractions. The size-dependent uncertainty associated to this parameter (variability due
218 to changes in ambient conditions and clogging of the air filters) was propagated during the
219 calculation of relative imbalance values. It is worth noting however that the penetration factor
220 showed stability over time for the smaller size bins corresponding to PM₁, which nonetheless
221 exhibit the strongest relative imbalance.

222 Size-resolved deposition rates (K) were derived after triggering a sharp increase in aerosol
223 concentrations (e.g. by vacuuming) and following its temporal decay, using the slopes of a linear
224 regression between the natural logarithm of particle number concentrations and time, subtracting
225 the air exchange rate (Equation 4).³⁷

$$226 \quad \ln[C_{in}(t) - C_{in,bkg}] = -(\alpha + K) \cdot t + \ln[C_{in}(0) - C_{in,bkg}] \quad \{4\}$$

227 where C_{in} and $C_{in,bkg}$ are the particle indoor and background concentrations ($\# \text{ m}^{-3}$), respectively,
228 α the air exchange rate (h^{-1}) and t the time (h). Given the complexity of generating large amounts
229 of particles within the whole volume of the room in all the relevant size bins, several criteria were
230 taken into consideration to ensure an accurate quantification of size-resolved PM deposition
231 rates: (i) a peak of particle number concentration during resuspension at least twice higher than
232 the background concentration for each size bin; (ii) a steady background, with a peak-to-peak
233 background fluctuation lower than 10% of the concentration enhancement during resuspension
234 for each size bin; (iii) a determination coefficient (r^2) higher than 0.9 for the linear regression
235 analysis (Eq. 4). Details on the deposition rate experiments are given in the SI.

236 **2.3. Size-resolved investigation of the aerosol budget indoors**

237 Simultaneous indoor and outdoor particle measurements were conducted on 24-hour periods
238 which were repeated 25 times during the campaign to investigate the aerosol budget indoors, that
239 is to say to characterize both sources and sinks and investigate mass closure under steady state
240 conditions. The dataset was screened for short-time windows (at least 1.5 h), characterized by
241 steady outdoor particle concentrations. A time window was considered suitable when the relative
242 standard deviation (RSD) of the measurements was less than 35%. This threshold was chosen to
243 ensure a statistically significant number of time windows for a robust analysis. Calculations using
244 other RSD thresholds ($< 35\%$) do not present improved results (Figure S3). Those short-time
245 windows allowed the application of the MBE, which otherwise would require to integrate the
246 measurements over significantly longer time-scales (days, weeks) to use the steady state
247 assumption.⁷⁵ Overall, 23 short-time windows (on 17 different days) were identified. The
248 parameter C_{out} was derived by averaging the outdoor concentration over the time windows while
249 C_{in} was averaged from the subsequent half hour (due to outdoor-indoor lag time discussed in

250 section 4 of the SI). All the other parameters required in Equation 1 were taken from the
251 characterization results described previously (α , P, K) and the geometry of the room (volume V).
252 Negligible resuspension (unoccupied room) and no direct emission or formation (empty room, no
253 human activities) were assumed for the MBE calculation as previously discussed.

254 3. Results

255 3.1. Size-resolved assessment of the MBE parameters

256 The average air exchange rate in the test room was $0.54 \pm 0.05 \text{ h}^{-1}$ (out of 9 experiments using
257 CO₂ time decays, see an example in section 5 of the SI). The values reported in the literature for
258 different types of buildings typically range from 0.12-3.5 h^{-1} under mechanically-ventilated
259 conditions, reaching up to 7.9 h^{-1} when air exchange is forced by the opening of windows and
260 doors^{23,76,77}. Our results show that air exchange is reasonably low, which is a feature of energy-
261 efficient buildings where heat loss is also minimized through reduced air exchange. In addition,
262 the air exchange rate calculated from the ventilation unit flow rate of $17 \text{ m}^3 \text{ h}^{-1}$ (value provided
263 by the manufacturer) and the room volume of 29.2 m^3 leads to a value of 0.58 h^{-1} (see section 5
264 of the SI). This value is in good agreement and falls within the uncertainties of the measured
265 AER of $0.54 \pm 0.05 \text{ h}^{-1}$. This excellent agreement (i) confirms the air flow rate of the ventilation
266 unit is stable over time, and (ii) supports our assumption to neglect air leakages.

267 Results for the penetration factor are shown in Figure 2, depicting a significant decrease with
268 increasing size (> 0.8 for PM₁ down to less than 0.2 for the coarse fraction). This trend, in
269 agreement with the literature,^{34,36,37,78,79} is expected since penetration depends on the particle size,
270 with fine particles ($< 2.5 \text{ }\mu\text{m}$) typically penetrating more easily than coarse ($> 2.5 \text{ }\mu\text{m}$) ones.
271 Other parameters influencing penetration factors are the chemical composition, phase state and

272 mixing state of particles,^{36,72,73} as well as the nature, thickness and shape of the filter, which may
273 explain some of the variability observed in the literature for each size bin (grey area in Figure 2).

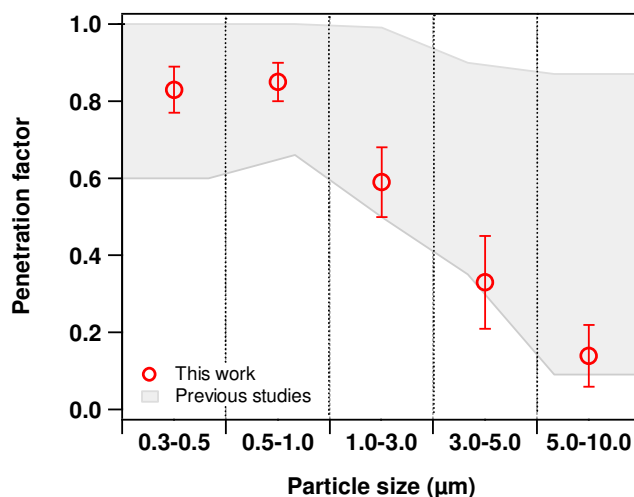


Figure 2: Average values of penetration factors (open markers) as a function of particle size. Error bars represent $\pm 1\sigma$ ($n = 235$). The shaded area represents the range of values obtained in previous studies.⁷²

274 Deposition rates were found to range from 0.2 h^{-1} up to 1.2 h^{-1} , as shown in Figure 3 and section
275 6 of the SI. Concentration levels reached upper values of 2.0×10^8 and 2.9×10^5 particles m^{-3} for
276 the smallest and largest size bins, respectively and each experiment lasted for 5-6 hours. The
277 lowest deposition rate was observed for 1.0-3.0 μm particles, and values reported for the different
278 size bin in this study are in agreement with previously reported deposition rates, although large
279 variability exists in the literature depending on room occupancy, air flow, aerosol type and
280 building materials.^{78,80} From Figure 3, and considering an air exchange rate of 0.5 h^{-1} , deposition
281 represents approximately one third, half and the total sink for particles smaller than 3.0 μm ,
282 ranging from 3.0-5.0 μm , and larger than 5 μm , respectively.

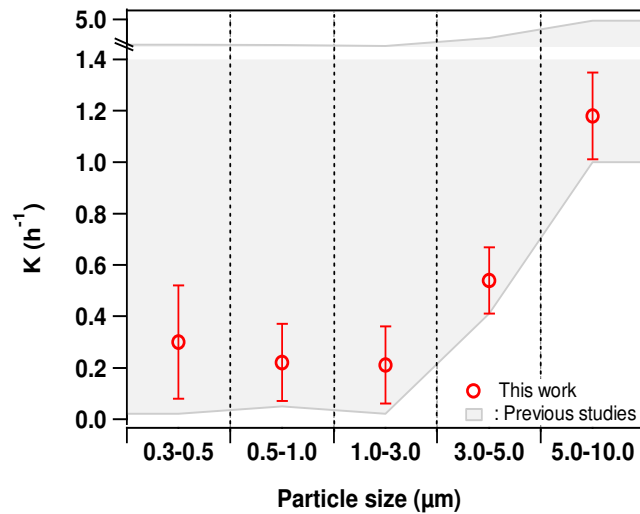


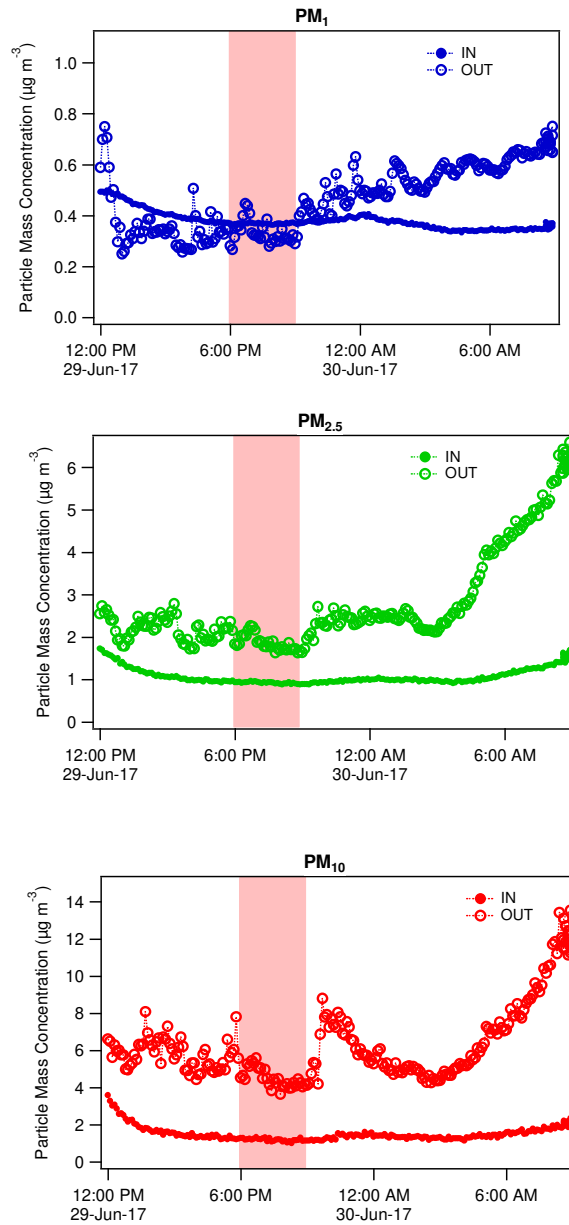
Figure 3: Average values of deposition rates (open markers) as a function of particle size. Error bars represent $\pm 1\sigma$ (9-15 measurements). The shaded area represents the range of values obtained in previous studies.^{37,78}

283 During deposition rate experiments, a three-fold increase was observed for submicron aerosols
 284 when ambient temperatures increased from 22°C to 29°C (Figure S7), a result that requires
 285 further analysis and, to the best of our knowledge, was not previously reported, although the
 286 influence of temperature gradients has been also suggested by Abt et al. (2000).⁸⁰

287 3.2. Indoor and outdoor particle concentrations

288 In Europe, the European Environmental Agency (EEA) and the World Health Organization
 289 (WHO)^{81,82} have regulated the PM₁₀ and PM_{2.5} fractions in ambient air, thus the mass
 290 concentrations of PM₁₀, PM_{2.5} (considered as particles with optical diameter below 3.0 μm for
 291 this study) and PM₁ were calculated assuming a spherical shape and an aerosol density of 1.4 g
 292 cm⁻³.⁸³ An example of indoor and outdoor particle concentrations is given in Figure 4 together
 293 with a time window selected for the mass budget analysis. The time series show that outdoor
 294 concentrations are highly variable due to the proximity of emission sources, while the indoor

295 concentration is buffered due to the slow air exchange rate and the absence of primary indoor
296 sources.



297 Figure 4: Example of time series of 6-minute averaged particle concentrations for the different
298 particle size fractions on 29-30 June 2017 measured indoor (filled) and outdoor (open circles). A

299 time window selected for mass budget analysis following the criteria described in subsection 2.3 is
300 highlighted in pink.

301 **4. Discussion**

302 **4.1. Impact of infiltration on indoor particle concentration**

303 Based on the air exchange rate and the size-resolved penetration factors and deposition rates, the
304 infiltration factor, i.e. the fraction of outdoor particles that penetrates and remains suspended
305 indoors, is defined as:

$$306 \quad F_{\text{inf}} = \frac{\alpha P}{\alpha + K} \quad \{5\}$$

307 and can be calculated considering an unoccupied room (particle sources and sinks only related to
308 air exchange and deposition). The indoor concentration of the finer fraction (0.3-0.5 μm) would
309 reach approximately 50% of the outdoor concentration, whereas for the 1.0-3.0 μm and 5.0-10.0
310 μm size bins this value would decrease to 43% and 4%, respectively. Such a marked decrease is
311 consistent with a combined effect of penetration factors decreasing with particle size and the
312 opposite behavior for deposition rates.

313 Actually, given that short-time windows were chosen under steady-state conditions, indoor
314 particle concentrations are always expected to be smaller than outdoor ones. While this was
315 observed to be true for particles larger than 1.0 μm , indoor PM_{10} concentrations were sometimes
316 similar to or even higher than outdoor ones, suggesting that processes other than penetration and
317 deposition are required to estimate concentrations of submicron particles in this unoccupied

318 room. The validity of the MBE for different particle sizes, including submicron particles, and
319 under different environmental conditions was therefore evaluated below.

320 **4.2. Evaluation of the relative imbalance for PM₁₀, PM_{2.5} and PM₁**

321 Under steady-state conditions in an unoccupied and empty room, the source and sink terms of the
322 MBE (Equation 1) should cancel each other out and PM concentrations should only depend on
323 the introduction of particles from outdoors (αPVC_{out}) and their loss through a combined effect of
324 air exchange and deposition ($(\alpha+K)VC_{in}$). In order to check this aspect, we define the Relative
325 Imbalance (RI) as the difference between source and sink rates, normalized to the source rate:

$$326 \quad RI = \frac{\alpha PVC_{out} - (\alpha + K)VC_{in}}{\alpha PVC_{out}} \quad \{6\}$$

327 Figure 5 depicts the averaged relative imbalance for the three PM fractions calculated for the 23
328 short-time windows during the campaign, with a distinction between warm ($T_{in} > 28$ °C, eight
329 time-windows) and cold ($T_{in} < 22$ °C, 15 time-windows) periods. This distinction has been
330 arbitrarily done based on the based on the observation of different results (in terms of RI) during
331 these two periods.

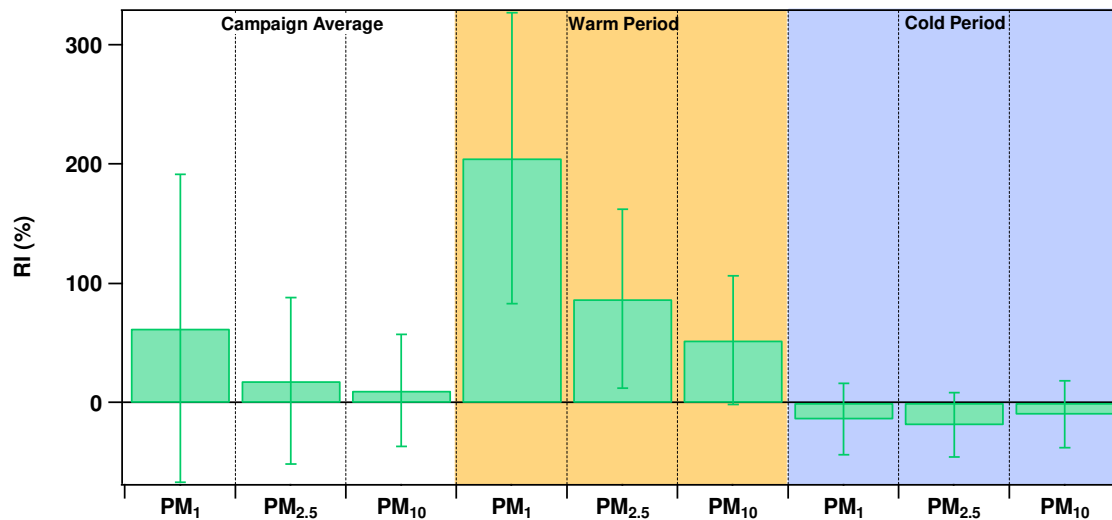


Figure 5: Averaged relative imbalance (RI; see equation 6) for the PM₁, PM_{2.5} and PM₁₀ size fractions (from left to right) considering the campaign average, warm periods only ($T_{in} > 28$ °C) and cold periods only ($T_{in} < 22$ °C). Error bars represent 1σ .

332 This figure shows that indoor PM₁₀ and PM_{2.5} concentrations are reasonably well estimated on a
 333 campaign average when both size-resolved penetration factors and deposition rates are correctly
 334 characterized (mean RI < 18%), whereas a larger variability is observed for RI on PM₁. A close
 335 look at the RI temporal variability for the three PM fractions indicates an important impact of
 336 temperature (Figures 5 and S8), with larger positive RI values at higher temperatures. This is also
 337 clearly depicted in Figure S8 (panel b), where RI values observed for each PM fraction during the
 338 warm period are larger than the means+ 1σ observed during the cold period (shaded area). These
 339 positive RI values indicate additional sources of PM in the building during the warm period,
 340 which are not observed during the cold period. It is interesting to note that the only parameter of
 341 the MBE that showed some temporal (or temperature) dependence was the deposition rate (more
 342 details in the SI), which was considered in this analysis. Not accounting for the larger deposition
 343 rates of PM₁ at higher temperatures would lead to even larger RI values for this PM fraction.

344 We speculate that different physicochemical processes, not accounted for in the mass balance
345 analysis performed above, are affecting the PM fractions. One assumption made in the above
346 analysis, similarly to other studies,^{42,60} is the negligible impact of resuspension on PM loading in
347 an unoccupied room. When temperature increases and relative humidity decreases, adhesive
348 forces between particles and surfaces become looser, thus an increase of resuspension rates can
349 impact the ambient PM concentrations. While this assumption may hold for the cold period,
350 higher ambient temperatures and lower relative humidity, can lead to an increase of resuspension
351 rates on hard floors (such as in this test room)⁸⁴ and, as a consequence, a significant impact of
352 resuspension on ambient PM concentrations. Interestingly, previous studies have shown that the
353 resuspension rate increases with particle size,^{31,32,38,84-86} indicating that resuspension rates for
354 PM₁ are orders of magnitude lower than for PM_{2.5} and PM₁₀. As a consequence, while an increase
355 of resuspension rates with temperature could explain the RI observed for PM_{2.5} and PM₁₀,
356 resuspension alone is unlikely to explain the larger RI observed for PM₁.

357 Additional physicochemical processes such as gas-to-particle conversion (condensation of low-
358 volatility gases) for particles smaller than 0.3 μm (lowest size measurable with the OPC) or the
359 reverse (volatilization of NH₄NO₃ or water soluble and semi-volatile organics)^{28,87-91} for particles
360 larger than 1 μm could also impact the PM₁ fraction. On one side, building materials covering
361 large surface areas in the building, mainly wood and linoleum, are known to emit monoterpenes
362 and SVOCs, respectively.⁹² Monoterpenes and other unsaturated VOCs are rapidly oxidized by
363 ozone, which in turn lead to the formation of oxygenated VOCs (OVOCs) of lower volatility. A
364 subsequent winter field campaign performed in the same test room (whose results are beyond the
365 scope of this publication but will be presented in a forthcoming paper) has shown that the total
366 concentration of the 60 measured OVOCs was at least eight times higher indoors (average C_{in} =

367 146.6 $\mu\text{g m}^{-3}$) compared to outdoors (average $C_{\text{out}} = 18.3 \mu\text{g m}^{-3}$), which supports that low-
368 volatility species could interact with the submicron aerosol population and could lead to a
369 modification of their size distribution. Besides, the emission of condensable gases from building
370 materials and gas-phase oxidation reactions are expected to become more significant at higher
371 temperatures (higher emission rates, higher ozone concentrations). On the other side,
372 volatilization of ammonium nitrate, leading to the formation of ammonia and nitric acid, has
373 already been observed indoors, with volatilization rates depending on temperature, relative
374 humidity and ventilation rate.²⁸ Both physicochemical processes (condensation and volatilization)
375 will be strongly linked to gas-particle equilibrium and temperature differences between indoors
376 and outdoors.

377 While the above discussion remains speculative, the results from this study indicate that
378 assuming no resuspension in an empty room seems to be a valid assumption for the use of the
379 mass balance model as long as ambient temperature remains under moderate values ($< 22^\circ\text{C}$ in
380 this study). Under these conditions, PM_x ($x = 1, 2.5, 10$) concentrations indoors can be accurately
381 assessed from outdoor measurements, providing that air exchange and deposition are well
382 characterized. However, this assumption may break down for higher temperatures, especially for
383 $\text{PM}_{2.5}$ and PM_{10} . In addition, the larger imbalance observed for PM_1 indicates that this PM
384 fraction is significantly more impacted by aerosol dynamics and thus requires a more detailed
385 knowledge of the complete aerosol size distribution, its physicochemical characteristics, and
386 physicochemical processes occurring indoors.

387 5. Conclusions

388 Particulate matter (PM) concentration indoors is the result of a balance between sources and
389 sinks, including potential physicochemical transformations, and a good understanding of these
390 processes is needed to correctly assess PM budget indoors. During this study the air exchange
391 rate, the penetration factor and deposition rates of size-resolved PM were measured in an
392 unoccupied energy-efficient building as defined by the French RT2012 regulation. Those
393 parameters were used to constrain a MBE linking indoor concentrations of PM to outdoor ones. It
394 was found that indoor concentrations of PM_x ($x = 1, 2.5, 10$) can be well estimated by the MBE
395 based on measured outdoor concentrations, as long as temperature does not exceed a certain
396 threshold of ambient temperatures (around 22°C in this study). In contrast, the indoor PM budget
397 was significantly less accurate, with measured indoor concentrations being up to four times
398 higher than values calculated from the mass balance approach for lower temperatures. This
399 disagreement is attributed on the one hand to the co-variability between processes and
400 transformations (gas-to-particle conversion, condensation, evaporation) taking place indoors for
401 the PM_1 fraction, and on the other hand to the assumed negligible resuspension mainly of coarse
402 particles ($PM_{2.5}$ and PM_{10}) even in a relatively source-free indoor environment.

403 The results of our study point out the limitations of a simplified mass balance analysis to estimate
404 PM fractions indoors, as can be classically found in the literature. It is usually assumed that under
405 unoccupied conditions the particles do not undergo transformations when they penetrate indoors.
406 Even under conditions where all the terms of the MBE have been carefully characterized and air
407 leakage is strongly minimized, such as in this work, this assumption leads to a miscalculation of
408 particle concentrations indoors during warm periods, whereas it seems to be accurate enough
409 (within uncertainties) for cold ones. Such results suggest that (i) the approximation of indoor

410 species as inert and (ii) the assumption of negligible resuspension are not valid depending on the
411 meteorological conditions, and an accurate budget analysis requires significantly more
412 sophisticated methodologies including a detailed chemical composition characterization of the
413 gas and particulate phases, even in a well-characterized and unoccupied environment.

414 **Acknowledgements**

415 We thank Dr. Serge Russeil from the Industrial Energy Department of IMT Lille Douai who
416 allowed the use of the energy-efficient building. E.Stratigou's PhD grant was funded by Armines.
417 IMT Lille Douai acknowledges financial support from the CaPPA project, which is funded by the
418 French National Research Agency (ANR) through the PIA (Programme d'Investissement
419 d'Avenir) under contract ANR-11-LABX-0005-01, and the CLIMIBIO project, both financed by
420 the Regional Council "Hauts-de-France" and the European Regional Development Fund (ERDF).

421 **References**

- 422 1. EPA. The total exposure assessment methodology (TEAM) study: Summary and
423 analysis. EPA/600/6-87/002a. Washington, DC. 1987.
- 424 2. WHO. *Burden of Disease from Household Air Pollution for 2016*. WHO Regional Office
425 for Europe; 2018. 2018. www.who.int.
- 426 3. Loomis D, Grosse Y, Lauby-Secretan B, et al. The carcinogenicity of outdoor air pollution.
427 *Lancet Oncol.* 2013;14:1262–1263.
- 428 4. Lanzinger S, Schneider A, Breitner S, et al. Associations between ultrafine and fine
429 particles and mortality in five central European cities — Results from the UFIREG study.
430 *Environ Int.* 2016;88:44–52.
- 431 5. Oberdörster G, Oberdörster E, Oberdörster J. Nanotoxicology: An Emerging Discipline
432 Evolving from Studies of Ultrafine Particles. *Environ Health Perspect.* 2005;113:823–839.
- 433 6. Pandis SN, Skyllakou K, Florou K, et al. Urban particulate matter pollution: a tale of five
434 cities. *Faraday Discuss.* 2016;189:277–290.

- 435 7. Destailhats H, Lunden M, Singer B, et al. Indoor Secondary Pollutants from Household
436 Product Emissions in the Presence of Ozone: A Bench-Scale Chamber Study. *Environ Sci*
437 *Technol.* 2006;40:4421–4428.
- 438 8. Rai AC, Guo B, Lin C-H, Zhang J, Pei J, Chen Q. Ozone reaction with clothing and its
439 initiated particle generation in an environmental chamber. *Atmos Environ.* 2013;77:885–
440 892.
- 441 9. Rai AC, Guo B, Lin C-H, Zhang J, Pei J, Chen Q. Ozone reaction with clothing and its
442 initiated VOC emissions in an environmental chamber. *Indoor Air.* 2014;24:49–58.
- 443 10. Waring MS, Siegel JA. Indoor Secondary Organic Aerosol Formation Initiated from
444 Reactions between Ozone and Surface-Sorbed d-Limonene. *Environ Sci Technol.*
445 2013;47:6341–6348.
- 446 11. Wang H, He C, Morawska L, McGarry P, Johnson G. Ozone-Initiated Particle Formation,
447 Particle Aging, and Precursors in a Laser Printer. *Environ Sci Technol.* 2012;46:704–712.
- 448 12. Fan Z, Weschler CJ, Han I-K, Zhang J (Jim). Co-formation of hydroperoxides and ultra-
449 fine particles during the reactions of ozone with a complex VOC mixture under simulated
450 indoor conditions. *Atmos Environ.* 2005;39:5171–5182.
- 451 13. Harb P, Sivachandiran L, Gaudion V, Thevenet F, Locoge N. The 40m³ Innovative
452 experimental Room for INdoor Air studies (IRINA): Development and validations. *Chem*
453 *Eng J.* 2016;306:568–578.
- 454 14. Rossignol S, Rio C, Ustache A, et al. The use of a housecleaning product in an indoor
455 environment leading to oxygenated polar compounds and SOA formation: Gas and
456 particulate phase chemical characterization. *Atmos Environ.* 2013;75:196–205.
- 457 15. Wierzbicka A, Bohgard M, Pagels JH, et al. Quantification of differences between
458 occupancy and total monitoring periods for better assessment of exposure to particles in
459 indoor environments. *Atmos Environ.* 2015;106:419–428.
- 460 16. Hovorka J, Braniš M. New particle formation and condensational growth in a large indoor
461 space. *Atmos Environ.* 2011;45:2736–2749.
- 462 17. Xiang J, Weschler CJ, Mo J, Day D, Zhang J, Zhang Y. Ozone, Electrostatic Precipitators,
463 and Particle Number Concentrations: Correlations Observed in a Real Office during
464 Working Hours. *Environ Sci Technol.* 2016;50:10236–10244.
- 465 18. Morawska L, He C, Johnson G, Guo H, Uhde E, Ayoko G. Ultrafine Particles in Indoor
466 Air of a School: Possible Role of Secondary Organic Aerosols. *Environ Sci Technol.*
467 2009;43:9103–9109.

- 468 19. Rim D, Choi J-I, Wallace LA. Size-Resolved Source Emission Rates of Indoor Ultrafine
469 Particles Considering Coagulation. *Environ Sci Technol*. 2016;0:null.
- 470 20. Patel S, Sankhyan S, Boedicker EK, et al. Indoor particulate matter during HOMEChem:
471 Concentrations, size distributions, and exposures. *Environ Sci Technol*. May 2020. May
472 11, 2020. <https://doi.org/10.1021/acs.est.0c00740>.
- 473 21. Polidori A, Turpin B, Meng QY, et al. Fine organic particulate matter dominates indoor-
474 generated PM_{2.5} in RIOPA homes. *J Expo Sci Environ Epidemiol*. 2006;16:321.
- 475 22. Hodas N, Turpin BJ. Shifts in the Gas-Particle Partitioning of Ambient Organics with
476 Transport into the Indoor Environment. *Aerosol Sci Technol*. 2014;48:271–281.
- 477 23. Farmer DK, Vance ME, Abbatt JPD, et al. Overview of HOMEChem: House Observations
478 of Microbial and Environmental Chemistry. *Environ Sci Process Impacts*. 2019;21:1280–
479 1300.
- 480 24. Johnson AM, Waring MS, DeCarlo PF. Real-time transformation of outdoor aerosol
481 components upon transport indoors measured with aerosol mass spectrometry. *Indoor Air*.
482 2017;27:230–240.
- 483 25. Lunderberg D, Kristensen K, Tian Y, et al. Surface emissions modulate indoor SVOC
484 concentrations through volatility-dependent partitioning. *Environ Sci Technol*. May 2020.
485 May 7, 2020. <https://doi.org/10.1021/acs.est.0c00966>.
- 486 26. Kopperud RJ, Ferro AR, Hildemann LM. Outdoor Versus Indoor Contributions to Indoor
487 Particulate Matter (PM) Determined by Mass Balance Methods. *J Air Waste Manag Assoc*.
488 2004;54:1188–1196.
- 489 27. Talbot N, Kubelová L, Makeš O, et al. Transformations of Aerosol Particles from an
490 Outdoor to Indoor Environment. *Aerosol Air Qual Res*. 2017;17:653–665.
- 491 28. Lunden MM, Revzan KL, Fischer ML, et al. The transformation of outdoor ammonium
492 nitrate aerosols in the indoor environment. *Indoor Air Chem Phys Pap Indoor Air 2002*.
493 2003;37:5633–5644.
- 494 29. Avery AM, Waring MS, DeCarlo PF. Seasonal variation in aerosol composition and
495 concentration upon transport from the outdoor to indoor environment. *Environ Sci Process*
496 *Impacts*. 2019.
- 497 30. Qian J, Ferro AR. Resuspension of Dust Particles in a Chamber and Associated
498 Environmental Factors. 2008;42:566–578.
- 499 31. Rosati JA, Thornburg J, Rodes C. Resuspension of particulate matter from carpet due to
500 human activity. *AEROSOL Sci Technol*. 2008;42:472–482.

- 501 32. Thatcher TL, Layton DW. Deposition, resuspension, and penetration of particles within a
502 residence. *Atmos Environ.* 1995;29:1487–1497.
- 503 33. Diapouli E, Chaloulakou A, Koutrakis P. Estimating the concentration of indoor particles
504 of outdoor origin: A review. *J Air Waste Manag Assoc.* 2013;63:1113–1129.
- 505 34. Thatcher TL, Lunden MM, Revzan KL, Sextro RG, Brown NJ. A Concentration Rebound
506 Method For Measuring Particle Penetration And Deposition In The Indoor Environment.
507 *Aerosol Sci Technol.* 2003;37:847–864.
- 508 35. Thatcher TL, Lai ACK, Moreno-Jackson R, Sextro RG, Nazaroff WW. Effects of room
509 furnishings and air speed on particle deposition rates indoors. *Atmos Environ.*
510 2002;36:1811–1819.
- 511 36. Long CM, Suh HH, Catalano PJ, Koutrakis P. Using Time- and Size-Resolved Particulate
512 Data To Quantify Indoor Penetration and Deposition Behavior. *Environ Sci Technol.*
513 2001;35:2089–2099.
- 514 37. Chao CYH, Wan MP, Cheng ECK. Penetration coefficient and deposition rate as a
515 function of particle size in non-smoking naturally ventilated residences. *Atmos Environ.*
516 2003;37:4233–4241.
- 517 38. Wang S, Zhao B, Zhou B, Tan Z. An experimental study on short-time particle
518 resuspension from inner surfaces of straight ventilation ducts. *Build Environ.*
519 2012;53:119–127.
- 520 39. Hussein T, Hruška A, Dohányosová P, et al. Deposition rates on smooth surfaces and
521 coagulation of aerosol particles inside a test chamber. *Atmos Environ.* 2009;43:905–914.
- 522 40. Hussein T, Korhonen H, Herrmann E, Hämeri K, Lehtinen KEJ, Kulmala M. Emission
523 Rates Due to Indoor Activities: Indoor Aerosol Model Development, Evaluation, and
524 Applications. *Aerosol Sci Technol.* 2005;39:1111–1127.
- 525 41. Talbot N, Kubelova L, Makes O, et al. Outdoor and indoor aerosol size, number, mass and
526 compositional dynamics at an urban background site during warm season. *Atmos Environ.*
527 2016;131:171–184.
- 528 42. Tran DT, Alleman LY, Coddeville P, Galloo J-C. Indoor particle dynamics in schools:
529 Determination of air exchange rate, size-resolved particle deposition rate and penetration
530 factor in real-life conditions. *Indoor Built Environ.* 2015;26:1335–1350.
- 531 43. Kopperud RJ, Ferro AR, Hildemann LM. Outdoor Versus Indoor Contributions to Indoor
532 Particulate Matter (PM) Determined by Mass Balance Methods. *J Air Waste Manag Assoc.*
533 2004;54:1188–1196.

- 534 44. Hussein T, Wierzbicka A, Löndahl J, Lazaridis M, Hänninen O. Indoor aerosol modeling
535 for assessment of exposure and respiratory tract deposited dose. *Atmos Environ.*
536 2015;106:402–411.
- 537 45. Zhu Y, Hinds WC, Krudysz M, Kuhn T, Froines J, Sioutas C. Penetration of freeway
538 ultrafine particles into indoor environments. *J Aerosol Sci.* 2005;36:303–322.
- 539 46. Chan WR, Logue JM, Wu X, et al. Quantifying fine particle emission events from time-
540 resolved measurements: Method description and application to 18 California low-income
541 apartments. *Indoor Air.* 2017;28:89–101.
- 542 47. Abt E, Suh HH, Catalano P, Koutrakis P. Relative Contribution of Outdoor and Indoor
543 Particle Sources to Indoor Concentrations. *Environ Sci Technol.* 2000;34:3579–3587.
- 544 48. Liu DL, Nazaroff WW. Particle Penetration Through Building Cracks. *Aerosol Sci*
545 *Technol.* 2003;37:7:565–573.
- 546 49. Mosley RB, Greenwell DJ, Sparks LE, et al. Penetration of Ambient Fine Particles into the
547 Indoor Environment. *Aerosol Sci Technol.* 2001;34:127–136.
- 548 50. Byrne MA, Goddard AJH, Lange C, Roed J. Stable tracer aerosol deposition
549 measurements in a test chamber. *J Aerosol Sci.* 1995;26:645–653.
- 550 51. Fogh CL, Byrne MA, Roed J, Goddard AJH. Size specific indoor aerosol deposition
551 measurements and derived I/O concentrations ratios. *Atmos Environ.* 1997;31:2193–2203.
- 552 52. Li Y, Chen Z. A balance-point method for assessing the effect of natural ventilation on
553 indoor particle concentrations. *Atmos Environ.* 2003;37:4277–4285.
- 554 53. Wallace L, Kindzierski W, Kearney J, MacNeill M, Héroux M-È, Wheeler AJ. Fine and
555 Ultrafine Particle Decay Rates in Multiple Homes. *Environ Sci Technol.* 2013;47:12929–
556 12937.
- 557 54. Stephens B, Siegel JA. Penetration of ambient submicron particles into single-family
558 residences and associations with building characteristics. *Indoor Air.* 2012;22:501–513.
- 559 55. Rim D, Wallace L, Persily A. Infiltration of Outdoor Ultrafine Particles into a Test House.
560 *Environ Sci Technol.* 2010;44:5908–5913.
- 561 56. Abt E, Suh HH, Allen G, Koutrakis P. Characterization of indoor particle sources: A study
562 conducted in the metropolitan Boston area. *Environ Health Perspect.* 2000;108:35–44.
- 563 57. Rim D, Choi J-I, Wallace LA. Size-Resolved Source Emission Rates of Indoor Ultrafine
564 Particles Considering Coagulation. *Environ Sci Technol.* 2016;0:null.

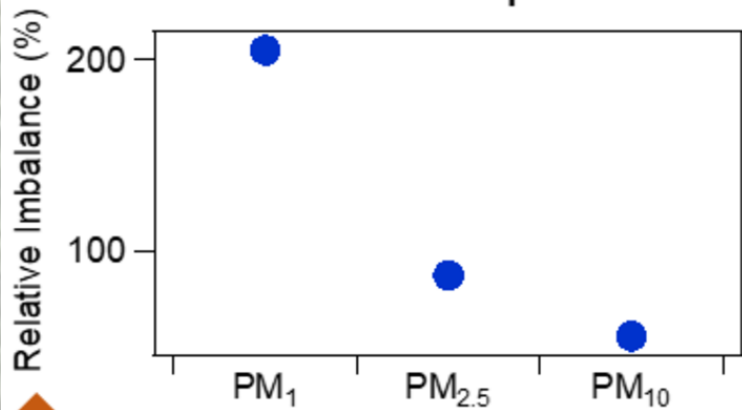
- 565 58. Waring MS. Secondary organic aerosol in residences: predicting its fraction of fine particle
566 mass and determinants of formation strength. *Indoor Air*. 2014;24:376–389.
- 567 59. Polidori A, Turpin B, Meng QY, et al. Fine organic particulate matter dominates indoor-
568 generated PM_{2.5} in RIOPA homes. *J Expo Sci Environ Epidemiol*. 2006;16:321.
- 569 60. Riley WJ, McKone TE, Lai ACK, Nazaroff WW. Indoor Particulate Matter of Outdoor
570 Origin: Importance of Size-Dependent Removal Mechanisms. *Environ Sci Technol*.
571 2002;36:200–207.
- 572 61. Chithra VS, Nagendra SMS. Indoor air quality investigations in a naturally ventilated
573 school building located close to an urban roadway in Chennai, India. *Build Environ*.
574 2012;54:159–167.
- 575 62. Wierzbicka A, Bohgard M, Pagels JH, et al. Quantification of differences between
576 occupancy and total monitoring periods for better assessment of exposure to particles in
577 indoor environments. *Atmos Environ*. 2015;106:419–428.
- 578 63. Hodas N, Turpin BJ. Shifts in the Gas-Particle Partitioning of Ambient Organics with
579 Transport into the Indoor Environment. *Aerosol Sci Technol*. 2014;48:271–281.
- 580 64. Farmer DK. Analytical Challenges and Opportunities For Indoor Air Chemistry Field
581 Studies. *Anal Chem*. 2019;91:3761–3767.
- 582 65. Johnson AM, Waring MS, DeCarlo PF. Real-time transformation of outdoor aerosol
583 components upon transport indoors measured with aerosol mass spectrometry. *Indoor Air*.
584 2017;27:230–240.
- 585 66. Lunden MM, Revzan KL, Fischer ML, et al. The transformation of outdoor ammonium
586 nitrate aerosols in the indoor environment. *Indoor Air Chem Phys Pap Indoor Air 2002*.
587 2003;37:5633–5644.
- 588 67. Chan WR, Logue JM, Wu X, et al. Quantifying fine particle emission events from time-
589 resolved measurements: Method description and application to 18 California low-income
590 apartments. *Indoor Air*. 2017;28:89–101.
- 591 68. Chithra VS, Nagendra SMS. Characterizing and predicting coarse and fine particulates in
592 classrooms located close to an urban roadway. *J Air Waste Manag Assoc*. 2014;64:945–
593 956.
- 594 69. Les économies d'énergie dans le bâtiment. February 6, 2020. [https://www.rt-
595 batiment.fr/batiments-neufs/reglementation-thermique-2012/presentation.html](https://www.rt-batiment.fr/batiments-neufs/reglementation-thermique-2012/presentation.html).
- 596 70. Weschler CJ, Carslaw N. Indoor Chemistry. *Environ Sci Technol*. 2018;52:2419–2428.

- 597 71. ASTM E 741 –00. Standard Test Method for Determining Air Change in a Single Zone by
598 Means of a Tracer Gas Dilution. 2006.
- 599 72. Chen C, Zhao B. Review of relationship between indoor and outdoor particles: I/O ratio,
600 infiltration factor and penetration factor. *Atmos Environ*. 2011;45:275–288.
- 601 73. Liu DL, Nazaroff WW. Particle Penetration Through Building Cracks. *Aerosol Sci*
602 *Technol*. 2003;37:7:565–573.
- 603 74. Chen C, Zhao B. Review of relationship between indoor and outdoor particles: I/O ratio,
604 infiltration factor and penetration factor. *Atmos Environ*. 2011;45:275–288.
- 605 75. Sun Z, Liu C, Zhang Y. Evaluation of a steady-state method to estimate indoor PM2.5
606 concentration of outdoor origin. *Build Environ*. 2019;161:106243.
- 607 76. You Y, Niu C, Zhou J, et al. Measurement of air exchange rates in different indoor
608 environments using continuous CO2 sensors. *J Environ Sci*. 2012;24:657–664.
- 609 77. Guo H, Morawska L, He C, Gilbert D. Impact of ventilation scenario on air exchange rates
610 and on indoor particle number concentrations in an air-conditioned classroom. *Atmos*
611 *Environ*. 2008;42:757–768.
- 612 78. Tran DT, Alleman LY, Coddeville P, Galloo J-C. Indoor particle dynamics in schools:
613 Determination of air exchange rate, size-resolved particle deposition rate and penetration
614 factor in real-life conditions. *Indoor Built Environ*. 2015;26:1335–1350.
- 615 79. Stephens B, Siegel JA. Penetration of ambient submicron particles into single-family
616 residences and associations with building characteristics. *Indoor Air*. 2012;22:501–513.
- 617 80. Abt E, Suh HH, Catalano P, Koutrakis P. Relative Contribution of Outdoor and Indoor
618 Particle Sources to Indoor Concentrations. *Environ Sci Technol*. 2000;34:3579–3587.
- 619 81. WHO. Air quality guidelines for particulate matter, ozone, nitrogen dioxide and sulfur
620 dioxide, Summary of risk assessment. 2005.
- 621 82. European Environmental Agency. *Air Quality in Europe*. 2016. <http://europa.eu>.
- 622 83. Rissler J, Nordin EZ, Eriksson AC, et al. Effective Density and Mixing State of Aerosol
623 Particles in a Near-Traffic Urban Environment. *Environ Sci Technol*. 2014;48:6300–6308.
- 624 84. Tian Y, Sul K, Qian J, Mondal S, Ferro AR. A comparative study of walking-induced dust
625 resuspension using a consistent test mechanism. *Indoor Air*. 2014;24:592–603.
- 626 85. Qian J, Peccia J, Ferro AR. Walking-induced particle resuspension in indoor environments.
627 *Atmos Environ*. 2014;89:464–481.

- 628 86. Salimifard P, Rim D, Gomes C, Kremer P, Freihaut JD. Resuspension of biological
629 particles from indoor surfaces: Effects of humidity and air swirl. *Sci Total Environ.*
630 2017;583:241–247.
- 631 87. Arhami M, Minguillón MC, Polidori A, Schauer JJ, Delfino RJ, Sioutas C. Organic
632 compound characterization and source apportionment of indoor and outdoor quasi-ultrafine
633 particulate matter in retirement homes of the Los Angeles Basin. *Indoor Air.* 2010;20:17–
634 30.
- 635 88. Matsumoto K, Ishii Y, Kim S, Kaneyasu N, Kobayashi H. Volatility of water-soluble
636 organic carbon in ambient aerosols. *J Aerosol Sci.* 2014;67:38–47.
- 637 89. Moreau-Guigon E, Alliot F, Gaspéri J, et al. Seasonal fate and gas/particle partitioning of
638 semi-volatile organic compounds in indoor and outdoor air. *Atmos Environ.*
639 2016;147:423–433.
- 640 90. Sangiorgi G, Ferrero L, Ferrini BS, et al. Indoor airborne particle sources and semi-volatile
641 partitioning effect of outdoor fine PM in offices. *Atmos Environ.* 2013;65:205–214.
- 642 91. Liu C, Zhang Y, Weschler CJ. The impact of mass transfer limitations on size distributions
643 of particle associated SVOCs in outdoor and indoor environments. *Sci Total Environ.*
644 2014;497–498:401–411.
- 645 92. Schripp T, Langer S, Salthammer T. Interaction of ozone with wooden building products,
646 treated wood samples and exotic wood species. *Atmos Environ.* 2012;54:365–372.

Energy Efficient Building

Mass balance equation



Deposition /
Resuspension

Air exchange

Penetration